Published in final edited form as:
Med Biol Eng Comput. 2008 April ; 46(4): 363–371. doi:10.1007/s11517-008-0311-5.

Multi-plug insole design to reduce peak plantar pressure on the diabetic foot during walking

Ricardo L. Actis[1], **Liliana B. Ventura**[1], **Donovan J. Lott**[2,3], **Kirk E. Smith**[2], **Paul K. Commean**[2], **Mary K. Hastings**[2,3], and **Michael J. Mueller**[2,3]

1*Engineering Software Research & Development, Inc.*

2*Washington University School of Medicine*

3*Program in Physical Therapy*

Abstract

There is evidence that appropriate footwear is an important factor in the prevention of foot pain in otherwise healthy people or foot ulcers in people with diabetes and peripheral neuropathy. A standard care for reducing forefoot plantar pressure is the utilization of orthotic devices such as total contact inserts (TCI) with therapeutic footwear. Most neuropathic ulcers occur under the metatarsal heads, and foot deformity combined with high localized plantar pressure, appear to be the most significant factors contributing to these ulcers. In this study, patient-specific finite element models of the second ray of the foot were developed to study the influence of TCI design on peak plantar pressure (PPP) under the metatarsal heads. A typical full contact insert was modified based on the results of finite element analyses, by inserting 4 mm diameter cylindrical plugs of softer material in the regions of high pressure. Validation of the numerical model was addressed by comparing the numerical results obtained by the finite element method with measured pressure distribution in the region of the metatarsal heads for a shoe and TCI condition. Two subjects, one with a history of forefoot pain and one with diabetes and peripheral neuropathy, were tested in the laboratory while wearing therapeutic shoes and customized inserts. The study showed that customized inserts with softer plugs distributed throughout the regions of high plantar pressure reduced the PPP over that of the TCI alone. This supports the outcome as predicted by the numerical model, without causing edge effects as reported by other investigators using different plug designs, and provides a greater degree of flexibility for customizing orthotic devices than current practice allows.

Keywords

Finite element analysis; diabetic foot; insole design

Introduction

High peak plantar pressures (PPP) during walking can contribute to painfal forefoot syndromes (i.e., metatarsalgia) in otherwise healthy people, and to skin breakdown in people with diabetes and peripheral neuropathy. Peripheral neuropathy is a common underlying cause of foot ulcers in patients with diabetes because the lack of painful feedback allows unnoticed repetitive tissue injury to occur [1]. During walking, normal and shear stresses develop which may lead to

serious damage in the neuropathic foot. Normal stresses originate by the repetitive vertical pressure on the foot while shear stresses occur when deep tissue slides under superficial tissue. It is currently accepted that reduction of abnormally high PPP during walking helps in the prevention and treatment of neuropathic ulcerations [2,3]. In this research study, total contact inserts (TCI) were used as the offloading mechanism because multiple studies have shown that the addition of a TCI can reduce PPP 16−48% under the metatarsal heads [4-8) compared to therapeutic footwear alone. The primary goal of the insert is to redistribute the plantar pressure from one specific location to a broader area [4,5].

A number of investigators have used finite element analysis to help design orthotic devices with the goal of reducing PPP. Research by other investigators include a partial 2D-model of the 2nd metatarsal region of the foot to study the effect on plantar pressure due to changes in insole and tissue thickness [9]; a 3D-model of the standing foot to study the effect of flat and conforming insole of different materials in the plantar pressure distribution [10,11]; a 2D-model of the heel region of the foot to study the effect that shape, material properties and thickness of the insole have on PPP [12]; a similar partial model of the 2nd metatarsal described by Lemmon et al. [9] to investigate the effect of softer single plugs of different shapes penetrating the complete thickness of the shoe midsole [13].

Given the proven effectiveness of the TCI design and the previous finite element model predictions, the aim of this study was to investigate various design modifications to further reduce the PPP beyond that of the standard TCI and single plug design. Numerical studies using our previously validated model [14] were performed to determine the influence of different TCI design configurations on the pressure distribution and peak pressure under the second metatarsal head during simulated push-off stance. We hypothesized that multiple small soft plugs placed under the metatarsal heads at the location of highest pressure would reduce these localized high PPP equivalent to a large single plug of material, with the added advantage of providing extra flexibility in TCI customization. The design of the TCI was changed by incorporating plugs of softer material in the regions of peak pressure and the numerical analysis repeated to determine the new pressure distributions. The design with the lowest peak pressure was determined numerically and prototype TCI inserts were manufactured to replicate this design. Their efficacy was tested using two subjects with high localized forefoot pressures to ascertain if the experimental observations were consistent with the numerical predictions.

Methods

Numerical simulation

The structure of the right foot used for the finite element model was generated from Spiral X-ray Computed Tomography (SXCT) image data [15] acquired while the subject was seated in a loading device and applying a load of 50% of body weight to the forefoot as described in detail elsewhere [14,16]. Briefly, the boundary coordinates were extracted from the SXCT data using the Analyze software system [17] and the pressure distribution was measured using the F-Scan system (Tekscan, South Boston, MA) with the pressure sensor taped to the plantar aspect of the subject's foot. The structure of the foot was characterized by bone, cartilage, flexor tendon, fascia and tissue. Figure 1 shows the individual two-dimensional models in the sagittal plane as developed for metatarsal 2 in the simulated push-off position using the finite element analysis program StressCheck (Engineering Software Research & Development, Inc., St. Louis, MO). Linear elastic material properties were used for bones $E = 7300$ MPa [18], cartilage $E = 10$ MPa [19], flexor tendon $E = 15$ MPa [20-22], and fascia $E = 85$ MPa [22]. Muscle and fat were grouped into a single material type (tissue) with nonlinear elastic properties characterized by a strain energy density function as reported in [14]:

$$W=W_L e^{2CW_L}, \qquad W_L=\frac{1}{2}\{\varepsilon\}^T [D] \{\varepsilon\} \tag{1}$$

where W is the strain energy density, W_L is the linear strain energy, C is a constant, e is te base of the natural logarithm, [D] is the linear stiffness matrix and {ε} is the strain tensor. This strain energy density function depends on three parameters: E (slope of the one-dimensionai stress-strain curve at ε=0), ν (Poisson's ratio), and C (constant with units of length^2/force). The values used for the material coefficients were E=0.30 MPa, C=60 MPa^{-1}, ν =0.45 as reported in [14]. Nonlinear material properties were specified for the standard TCI (#2 plastizote), the softer plugs (Poron) and shoe sole (rubber). The material properties for rubber and plastizote were obtained by compression testing of samples taken from the shoe sole and insert [14] utilizing an Instron testing machine (Wilson Instruments, Canton, MA) and following the procedures described in the ASTM standard D575−91, while those of the Poron were obtained from the literature [13]. For the TCI and plugs, a 5-parameter nonlinear material description was used, characterized by the slope of the initial linear portion (E), the Poisson's ratio (v), the strain at the end of the linear range (ε_1), the slope of a second linear region (Et), the starting point on the second linear part of the stress-strain relationship given by the strain (ε_2) and the corresponding stress (σ_2). The stress-strain law is linear for strains less than ε_1 and for strains greater than ε_2. The two linear segments are joined by a cubic spline. The following values were used for the #2 plastizote: E=1.75 MPa, Et=0.0175 MPa, ε_1=0.046, ε_2=0.2, σ_2=0.105 MPa, v=0.2, and Poron: E=0.80 MPa, Et=0.13 MPa, ε_1=0.031, ε_2=0.1, σ_2=0.05 MPa, v=0.3. The corresponding stress-strain curves are shown in Figure 2. Testing was conducted to 0.30 strain because greater strains in the shoe insole or total contact insert (plastizote) were not observed during the unloaded to loaded CT scans. In addition, we did not test the plastizote greater than 30% deformation because greater strain would result in permanent deformation. For the shoe sole, the strain energy density function given by equation (1) was used with values: E=1.25 MPa, C=25 MPa^{-1}, ν =0.45.

A compression load was applied to the tibia and a moment was added to incorporate the compensating effect of the Achilles tendon (not included in the model). The flexor tendon was pre-stressed to represent typical values found in the literature for the Flexor Digitorum Longus during push-off [23].

The finite element mesh density was selected to capture the topological complexity of the model and frictionless contact condition was specified between the foot and the TCI. The elements representing the TCI were directly connected to those representing the sole of the shoe. The shoe was supported with a compression-only elastic foundation (no friction) with an elastic constant selected to represent the stiffness of the support plate in the loading device. Plane strain conditions were assumed.

The numerical solution was obtained by increasing the polynomial degree of elements (p-level) on a fixed mesh. A sequence of contact solutions was obtained for several p-levels until the estimated relative error in energy norm [24] was small (under 2%), followed by a nonlinear analysis to incorporate the effects of material nonlinearities and subsequent modification of the contact. Validation of the numerical model was addressed by comparing the numerical results obtained by the finite element method with measured pressure distribution with the F-Scan system in the region of the metatarsal heads for a shoe and TCI condition [14].

For the model validation, the pressure distribution for the barefoot and standard condition footwear of a diabetic subject was obtained from the FEA model and compared with the pressure distribution obtained from the F-Scan system. The F-Scan pressure recording was made while the subject was sitting in the loading device and applying a load of 50% of body

weight to their forefoot. Previous work has demonstrated that the forefoot pressure distribution collected with the subject sitting on the loading device is similar to the forefoot pressure distribution at the instant of peak pressure during the push-off phase of walking (80% of stance phase) [14-15]. The results of the FEA model and experimental pressure testing were in good agreement. For example, Figure 3 shows the pressure distribution for the 2nd ray – barefoot and footwear conditions - measured and calculated (r=0.83 for barefoot and r=0.95 for shoe and TCI). For the initial FEA, the 2nd ray was loaded with 75 N which was equivalent to 20% of the total foot load measured during pressure and structure data acquisition on the loading device for that specific subject [14]. A specific model also was developed for the diabetic subject tested in this study using a load of 62 N which was equivalent to 20% of his total foot load measured during his data acquisition. A specific model was not made for the subject with metatarsalgia because structure data was not available for him.

Once the numerical model was validated, several design changes were incorporated in the TCI to reduce the peak plantar pressure further from that of the TCI alone.

TCI Design Modifications

One way to further reduce the peak plantar pressure (PPP) over that of the TCI insole alone is to insert soft plugs in the regions of high PPP. When a single soft plug is inserted through the complete thickness of the TCI, the softer material of the plug comes into direct contact with the sole of the foot. This creates a potential problem because of the stiffness discontinuity at the boundary between the softer plug and the rest of the insole. It has been reported that localized high plantar pressure may develop in this region depending on the configuration of the plugs [13].

To avoid the stiffness discontinuity problemn and to provide a more flexible design solution we propose a different strategy to locally reduce the stiffness of the TCI in the regions of PPP. The modification consists of inserting several small-diameter cylindrical plugs of softer material in the regions of high pressure with partial penetration through the thickness so as not to reach the side of the TCI in contact with the foot (see detail in Figure 1), but deep enough to provide a pressure relief. We also investigated single plug configurations with a partial (box) or full penetration (plug) through the TCI to compare the results with the multi-plug design. Several design variations were considered during the numerical simulation including changes in the number of plugs (5−15), plug diameter (2−8 mm), distance between plugs (1−5 mm), plug height (50−100% thickness of TCI) and material properties (E=0.25−2.25 MPa). For each design configuration, a finite element analysis was performed for the 2nd ray model, and the performance of the design was compared with the standard plastizote TCI. An example of the comparison between 7, 8, or 9 cylinders and the TCI is illustrated in Figure 4. An example of the comparison between the cylinders, box, and plug designs is illustrated in Figure 5.

The best design (lowest peak pressure) of the tested configurations consisted of 4 mm diameter plugs with 1 mm separation that penetrated 70% through the thickness of the TCI. One plug was centered in the region of the PPP, 3 to 4 cylinders were placed proximally and 3 to 4 cylinders were placed distally from the point of PPP, for a total of 7 to 9 cylinders. Even though softer materials were considered for the plugs during the numerical simulation, because of its commercial availability, Poron (Acor, Inc., Cleveland, OH) was used for the construction of the soft plugs in the TCI prototypes.

The numerical analyses were repeated after modifying the standard TCI by inserting a Poron plug that was approximately 34 mm wide (equivalent to seven 4 mm diameter cylinders separated by 1 mm each) with a thickness that was 70% the thickness of the TCI (box) and again using a plug that was 34 mm wide and 100% the thickness of the TCI (plug) (Figure 5). The results of each numerical TCI alteration were compared with those obtained using the

standard TCI to determine which design offered the greatest pressure reduction. Prototypes were constructed and tested on two subjects (one subject with a history of forefoot pain and one subject with diabetes and peripheral neuropathy) during walking.

Prototype insoles

A set of four prototype insoles were constructed to fit a male volunteer (47 years old, 165 lb), with a history of forefoot pain (metatarsalgia), and a male volunteer with a history of diabetes and peripheral neuropathy (68 years old, 176 lb, 44 years of DM). These 2 subjects were selected from a larger study because they had high localized pressures in the forefoot that were not fully resolved from using a TCI alone. Both subjects signed an institutional review board approved consent form. First, a custom TCI insole of standard plastizote material, about 10 mm thick in the region of the metatarsal heads, was made to fit both the left and right feet of each subject as described previously [4]. Briefly, the certified orthotist took a foam impression of a subject's foot to make a positive plaster model of their foot. The foam was compressed 2 −4 cm to capture the entire impression of the foot and medial longitudinal arch. The TCI was made from a base of 1.27 cm (1/2") #2 plastizote with a shore value of approximately 35 and heightened to include the medial longitudinal arch fabricated to fit inside the shoe. A trial in-shoe pressure assessment using the F-Scan system was then performed with the subjects wearing the unmodified standard TCI and standard shoes. From the F-scan pressure reading corresponding to an instant during the late stance phase of walking (highest pressure in the forefoot region – Figure 6b & Figure 7b) and based on the results of the numerical studies, a Poron plug pattern was designed to extend approximately 15 mm proximally, distally, laterally and medially from the location of the PPP. The Poron plugs were 4 mm in diameter, spaced 1 mm apart extending in all direction around the point of PPP, and penetrated 7 mm into the TCI (local plug design – Figure 6c & Figure 7c). It is important to point out that the locations of the plugs were determined from the pressure readings and not from the location of the metatarsal heads [13]. Two additional patterns were also tested: one in which Poron plugs were placed throughout the entire forefoot region (global plug design – Figure 6d & Figure 7d), and the other in which a single 7 mm thick sheet of Poron was used in the forefoot region (inlay design – Figure 6e & Figure 7e). We tested both localized and global variations of the multiple plug design to determine if there was a benefit to widespread plug coverage, and we tested the inlay design because a similar design was modeled by Erdemir et al [13] and is often used in clinical practice.

Pressure Testing

Plantar pressures were recorded during walking in all 4 insole conditions (Figures 6 and 7) using the F-Scan system and previously validated methods [25-27]. A new F-scan pressure sensor was cut to fit the shoe of each subject, and the pressure sensor was placed in the footwear over the insole and under the plantar foot. Subjects wore their own socks and SoleTech shoes (style E3010). This footwear was selected because it is widely used in practice and can accommodate custom-made orthotic devices. The sensor was calibrated according to manufacturer guidelines and standardized techniques [26, 27] and the data was collected at 50 Hz during 6 walking trials immediately after calibration. A mean of 3 representative steps (not highest or lowest) was chosen during the mid portion of each walking trial and a mean of the 18 steps was used for the peak pressure. Order of testing for the 4 conditions was determined randomly using a prearranged schedule. Subjects were timed as they walked across a 6.1 meter (20 ft) walkway, but were allowed to walk at their preferred walking speed. Walking trials with speeds that differed by more than 5% between footwear conditions were repeated.

Results

Numerical analysis

Figure 4 shows the FEA results of the pressure distribution 35 mm proximal and 30 mm distal from the center of the metatarsal head of the 2nd ray of the diabetic subject for four conditions: standard plastizote TCI, TCI with 7 Poron plugs (7 cylinders), 8 Poron plugs (8 cylinders) and 9 Poron plugs (9 cylinders). In all the testing conditions using plugs, one plug is located at the position of the PPP for the standard TCI, and three plugs are placed proximally from it and 3, 4 or 5 plugs are placed distally to complete the design. The results show that the 7, 8 and 9-plug designs are more effective in reducing the PPP compared to the TCI alone, and that adding more plugs distally (9-plug design) reduces the secondary peak observed at about 20 mm distally from the center of the metatarsal head compared to the 7 plug design. Note that this secondary peak is not present for the standard TCI.

Figure 5 shows the FEA results of the pressure distribution 35 mm proximal and 30 mm distal from the center of the metatarsal head of the 2nd ray of the diabetic subject and for four conditions: standard plastizote TCI, TCI with 7 Poron plugs (cylinders), TCI with a single partial penetration Poron plug (Box) and TCI with a complete penetration Poron plug (Plug). All three designs have lower peak plantar pressure than the TCI alone (121 kPa). While the single plug design (PPP=106 kPa for Plug, PPP=107 kPa for Box) provides similar pressure reduction compared to the multi-plug design (PPP=110 kPa), the single plug designs produce an undesirable secondary pressure peak 20 mm distally from the center of the metatarsal head at the end of the plug.

Experimental measurements

Table 1 shows the average peak plantar pressure (PPP) for the four different regions of the forefoot (Figure 6b) and four different TCI conditions obtained from the F-Scan measurements for the subject with a history of metatarsalgia. The PPP and standard deviation (STD) values are averages over 18 steps. The last column in each region shows the percent change in pressure (ΔP) over that of the TCI alone (a positive number indicates a pressure increase, while a negative number a reduction in pressure). While each of the designs reduced PPP in the middle region (where initial PPP was highest and the subject had a history of pain) these results show that the local plug was the most effective in reducing the PPP in this targeted region (13.6% reduction from 427 kPa to 369 kPa). The local plug design also showed a reduction of PPP in the medial region of 11.4%, with a small increase in pressure in the lateral and great toe regions (4.6% and 3%, respectively).

Table 2 shows the same information for the subject with diabetes and peripheral neuropathy. In this case, the global plug and the local plug designs show a reduction in the PPP occurring in the middle and lateral regions (3.3−24.5%), while the inlay was not effective. There was a pressure increase in the great toe and medial regions for all three plug configurations, but the pressure for the standard TCI was less than in the other two regions.

Discussion

The present modeling approach is based on the use of subject-specific topologies for the foot and shoe to study the influence of design variations of the insert on the peak plantar pressure under the metataral heads and the correlation with experimental results obtained during walking.

In this research a two-dimensional validated model of the second ray was used to study the beneficial effect of incorporating small cylindrical plugs with partial penetration through the thickness of the insert in the areas where the plantar pressure is largest. The numerical

simulations made it possible to study different plug patterns without the difficulties associated with empirically testing all of these configurations. From the numerical studies of multiple configurations, the best plug configuration was determined and prototype inserts were made and tested experimentally in two subjects during walking.

Both subjects showed a reduction in peak pressure (Tables 1-2) that was consistent with the predicted values from the computational modeling (Figure 5). It is interesting to point out that although the reduction in PPP is less for the subject with diabetes and peripheral neuropathy than for the subject with a history of metatarslagia, the initial PPP with the TCI alone is substantially less for the subject with diabetes and therefore the pressure reduction provided by the plugs is not as effective as it is for the subject with a history of metatarsalgia.

Although a number of other investigators have used finite element models to design orthotic devices [9-13], the work of Erdemir et al is most pertinent to this project [13]. Erdemir et al investigated the shape and size of an individual plug placed within the midsole of the shoe. Our study differs in that we investigated number and distribution of plugs placed within a total contact insert (TCI) that could be placed inside the shoe. Both studies placed the plugs under the area of highest pressure rather than under the metatarsal heads because Erdemir et al found PPP were lower using this configuration. This approach intuitively makes sense and optimally requires an in-shoe pressure assessment prior to insole or footwear fabrication. Furthermore, both studies report an “edge effect” (i.e., a ridge of high pressure at the edge of the plug) using a single plug with vertical sides. Erdemir et al minimizes this potential problem by using a larger plug or by tapering the edges. We found that the edge effect could be lessened by using multiple smaller plugs. Finally, Erdemir et al reports larger PPP reductions in the region of interest predicted numerically (18−28% vs 7%) and experimentally (44−45% vs 3−14%) than we report. These considerably greater PPP reductions likely are due to the larger, thicker plugs used by Erdemir et al that were placed in the midsole of the shoe compared to the plugs used in this study that were inserted only into the insole.

A TCI clearly is beneficial in reducing forefoot PPP [4-8]. Although many patients receive adequate pressure reduction from the TCI alone, some patients require greater pressure reduction due to reoccurring pain or plantar ulcers. Traditionally, a metatarsal pad is used for further pressure reduction [4]. We believe the use of small plugs as a way to reduce the PPP further from that of the TCI alone may have several potential advantages. Using small plugs may: (a) provide greater flexibility (i.e., more options) for customizing therapeutic insoles-for each individual patient, and (b) avoid the possible detrimental effect of secondary pressure peaks at the transition between softer and stiffer materials of the total penetration plugs (Figure 5 - plug). Additional research is needed to compare these approaches directy.

Several limitations to our numerical approach need to be emphasized for appropriate interpretation and application of our results. First a static two dimensional model was used to characterize a dynamic three dimensional phenomena. A two dimensional model is unable to accurately identify the distribution of pressure across metatarsal heads. This limitation is especially important in trying to identify the benefits of a local compared to a global plug distribution. In addition, we characterized only one instant during the entire stance phase of walking. This instant during the push-off phase of walking was chosen, however, because it is the instant when pressures are greatest on the plantar foot and risk of injury is highest.[15] Although we used a loading device to position and load the foot during a simulated instant of push-off during walking, our previous research indicated that the pressure values collected on this loading device were representative of values collected during walking [15]. Furthermore, a frictionless contact condition was used between the foot and insole which is unable to identify shear stresses that may be harmful to the foot. We are unable to determine the effect of shear stresses on the plantar foot using this computational model. Despite these limitations, the two

dimensional model has been validated with experimental results [14] and helped select specific designs that were then tested in the laboratory and reported in this paper. The results of empirical tests (Tables 1-2) were consistent with the estimates derived from the model (Figure 5) increasing our confidence in the model predictions. Continued research is needed to develop validated dynamic three dimensional models of the foot that can help direct optimal footwear design for the serious problem of neuropathic skin breakdown.

This research study indicates that the use of softer localized plugs inserted into a monolithic TCI insole is a good strategy to reduce peak plantar pressure in the metatarsal region of the diabetic foot. The numerical simulations were essential in determining the proper size and number of plugs while the specific placement of the plugs was determined from pressure measurements made using an in-shoe pressure assessment system. Additional testing in larger groups of patients with high pressures resulting in forefoot pain or skin breakdown (i.e., from diabetes and peripheral neuropathy) is needed to confirm the benefits of the proposed approach.

Acknowledgements

We acknowledge funding from NCMRR, NIH, ROI RD 36895. We also acknowledge Mike Dailey, CPed CO, for fabricating orthotic devices used in this study.

Glossary

CT, Computed Tomography; DM, diabetes mellitus; FEA, finite element analysis; SXCT, spiral X-ray computed tomography; TCI, total contact insert; PPP, peak plantar pressure.

References

1. Pecoraro RE, Reiber GE, Burgess EM. Pathways to diabetic limb amputation. Basis for prevention. Diabet Care 1990;13(5):513–521.
2. Edmonds M, Blundell M, Morris M, et al. Improved Survival of the Diabetic Foot: The Role of a Specialized Foot Clinic. Q J Med 1986;60(232):763–771. [PubMed: 3774959]
3. Chantelau E, Haage P. An audit of cushioned diabetic footwear: relation to patient compliance. Diabet Med 1994;11(1):114–116. [PubMed: 8181241]
4. Mueller MJ, Lott DJ, Hastings MK, Commean PK, Smith KE, Pilgram HK. Efficacy and mechanism of orthotic devices to unload metatarsal heads in people with diabetes and a history of plantar ulcers. Phys Ther 2006;86(6):833–842. [PubMed: 16737409]
5. Bus SA, Ulbrecht JS, Cavanagh PR. Pressure relief and load redistribution by custom-made insoles in diabetc patients with neuropathy and foot deformity. Clin Biomech 2004;19(6):629–638.
6. Ashry HR, Lavery LA, Murdoch DP, Frolich M, Lavery DC. Effectiveness of diabetic insoles to reduce foot pressures. J Foot Ankle Surg 1997;36:268–271. [PubMed: 9298441]
7. Lord M, Hosein R. Pressure redistribution by molded inserts in diabetic footwear: a pilot study. J Rehabil Res Dev 1994;31(3):214–221. [PubMed: 7965879]
8. Tsung BYS, Zhang M, Mak AFT, Wong MWN. Effectiveness of insoles on plantar pressure redistribution. J Rehabil Res Dev 2004;41(6A):767–774. [PubMed: 15685465]
9. Lemmon D, Shiang TY, HIashmi A, Ulbrecht JS, Gavanlagh PR. The effect of insoles in therapeutic footwear – A finite element approach. J Biomech 1997;30−6:615–620.
10. Chen WP, Ju CW, Tang F. Effects of total contact insoles on the plantar stress distribution: a finite element analysis. Clin Biomech 2003;18:S17–S24.
11. Cheung JTM, Phil M, Zhang M. A three-dimensional finite element model of the human foot ans ankle for insole design. Arch Phys Med Rehabil 2005;88:353–358. [PubMed: 15706568]
12. Goske S, Erdemir A, Petre M, Budhabhatti S, Cavanagh PR. Reduction of plantar heel pressure: Insole design using finite element analysis. J Biomech 2005;39:2363–2370. [PubMed: 16197952]

13. Erdemir A, Saucerman JJ, Lemmon D, Loppnow B, Turso B, Ulbretch JS, Cavanagh PR. Local Pressure Relief in Therapeutic Footwear: Design Guidelines from Fminte Element Models. J Biomech 2005;38:1798–1806. [PubMed: 16023466]

14. Actis RL, Ventura LB, Smith KE, Commean PK, Lott DJ, Pilgrain TK, Mueller MJ. Numerical simulation of the plantar pressure distribution in the diabetic foot during the push-off stance. Med Bio Eng Comput 2006;44:653–663. [PubMed: 16937207]

15. Commean PK, Mueller MJ, Smith KE, Hastings M, Klaesner J, Pilgram T, Robertson DD. Reliability and Validity for Combined Inaging and Pressure Assessment Methods-for Diabetic Feet. Arch Phys Med Rehabil 2002;83(4):497–505. [PubMed: 11932851]

l6. Hastings MK, Commean PK, Smith KE, Pilgram TK, Mueller MJ. Aligning anatomical structure from spiral X-ray computed tomography with plantar pressure data. Clim Biomech 2003;18:877–882.

17. Robb RA, Barillot C. Interactive display and analysis of 3-D medical images. IEEE Transactions on Medical Inaging 1989;8(3):217–226.

18. Gefen A, Megido-Ravid M, Itzchak Y, Arcan M. Biomechanical Analysis of the Three-Dimensional Foot Structure during Gait: A Basic Tool for Clinical Applications. J Biomech Eng 2000;122:630–639. [PubMed: 11192385]

19. Jacob S, Patil MK. Stress Analysis in Three-Dimensional Foot Models of Normal and Diabetic Neuropathy. Frontiers of Medical & Biological Engineering 1999;9:211–227. [PubMed: 10612561]

20. Yamada, H. Strength of Biological Materials. The William & Wilkins Company; Baltimore: 1970.

21. Gefen A. Plantar Soft Tissue Loading under the Medial Metatarsals in the Standing Diabetic Foot. Med Eng Phys 2003;25:491–499. [PubMed: 12787987]

22. Gefen A. The In Vivo Elastic Properties of the Plantar Fascia during the Contact Phase of Walking. Foot and Ankle International 2003;24:238–244. [PubMed: 12793487]

23. Jacob S, Patil MK. Three-Dimensional Foot Modeling and Analysis of Stresses in Normal and Early Stage Hansen's Disease with Muscle Paralysis. J Rehabil Res Dev 1999;36:252–263. [PubMed: 10659808]

24. Szabo, BA.; Babuska, I. Finite Element Analysis. John Willey and Sons Inc.; New York: 1991.

25. Mueller MJ, Strube MJ. Generalizability of in-shoe peak pressure measures using the f-scan system. Clin Biomech 1996;11:159–164.

26. Nicolopoulos CS, Anderson EG, Solomonidis SE, Giannoudis PV. Evaluation of the gait analysis FSCAN pressure system: clinical tool or toy? Foot 2000;10:124–130.

27. Pitei DL, Lord M, Foster A, Wilson S, Watkins PJ, Edmonds ME. Plantar pressures are elevated in the neuroischemic and the neuropaic diabetic foot. Diab Care 1999;22(12):1966–1970.

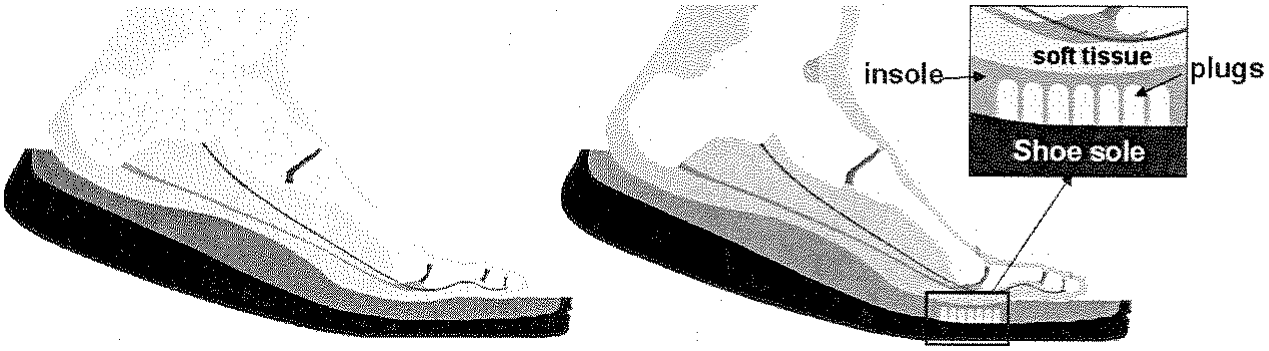

Figure 1.
2nd ray – sagittal plane section used for numerical simulation. Foot with standard TCI (left) and with plugs under the metatarsal head (right). Inset shows detail of plug design.

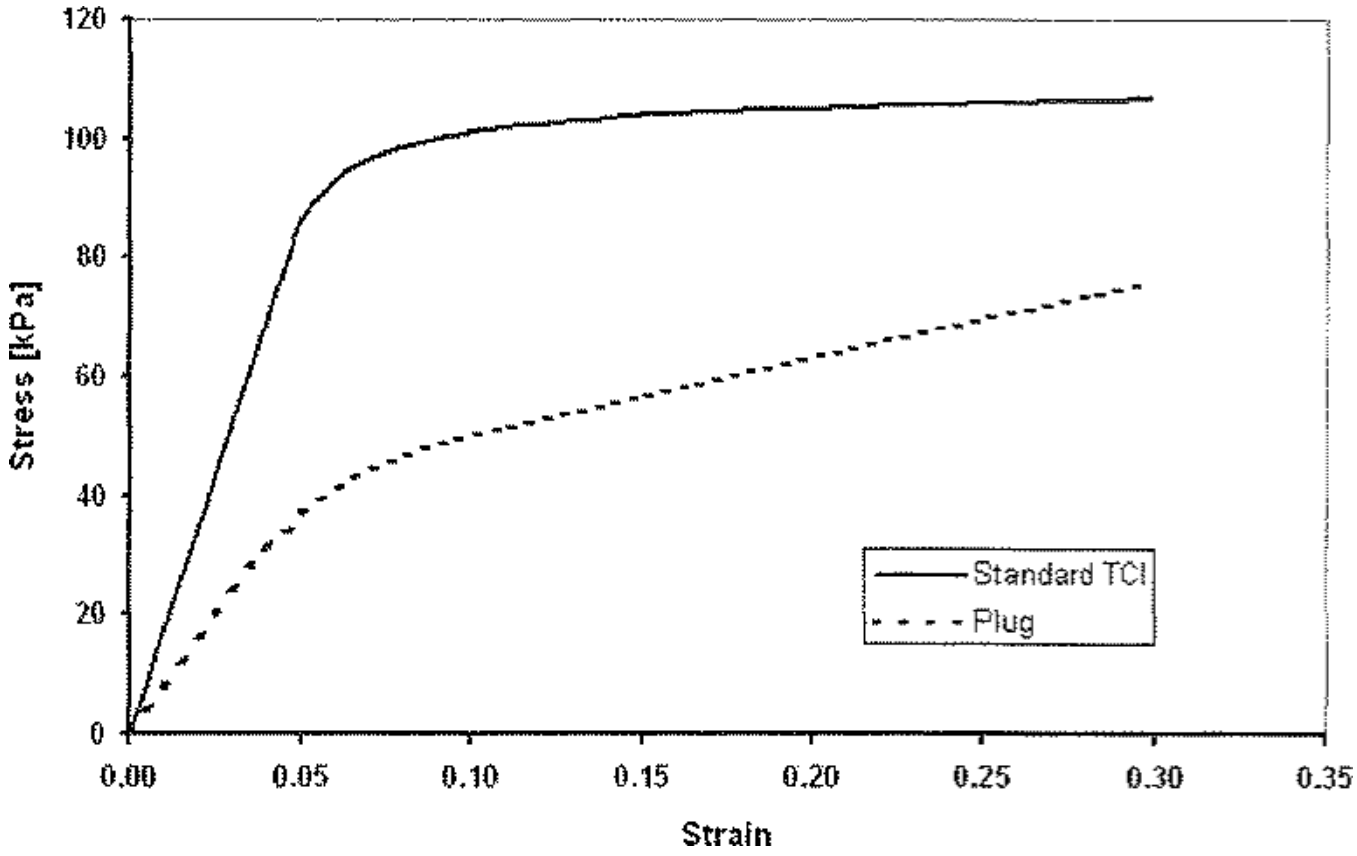

Figure 2.
Stres-strain curves for the standard TCI (pastizote #2) and plug material (Poron).

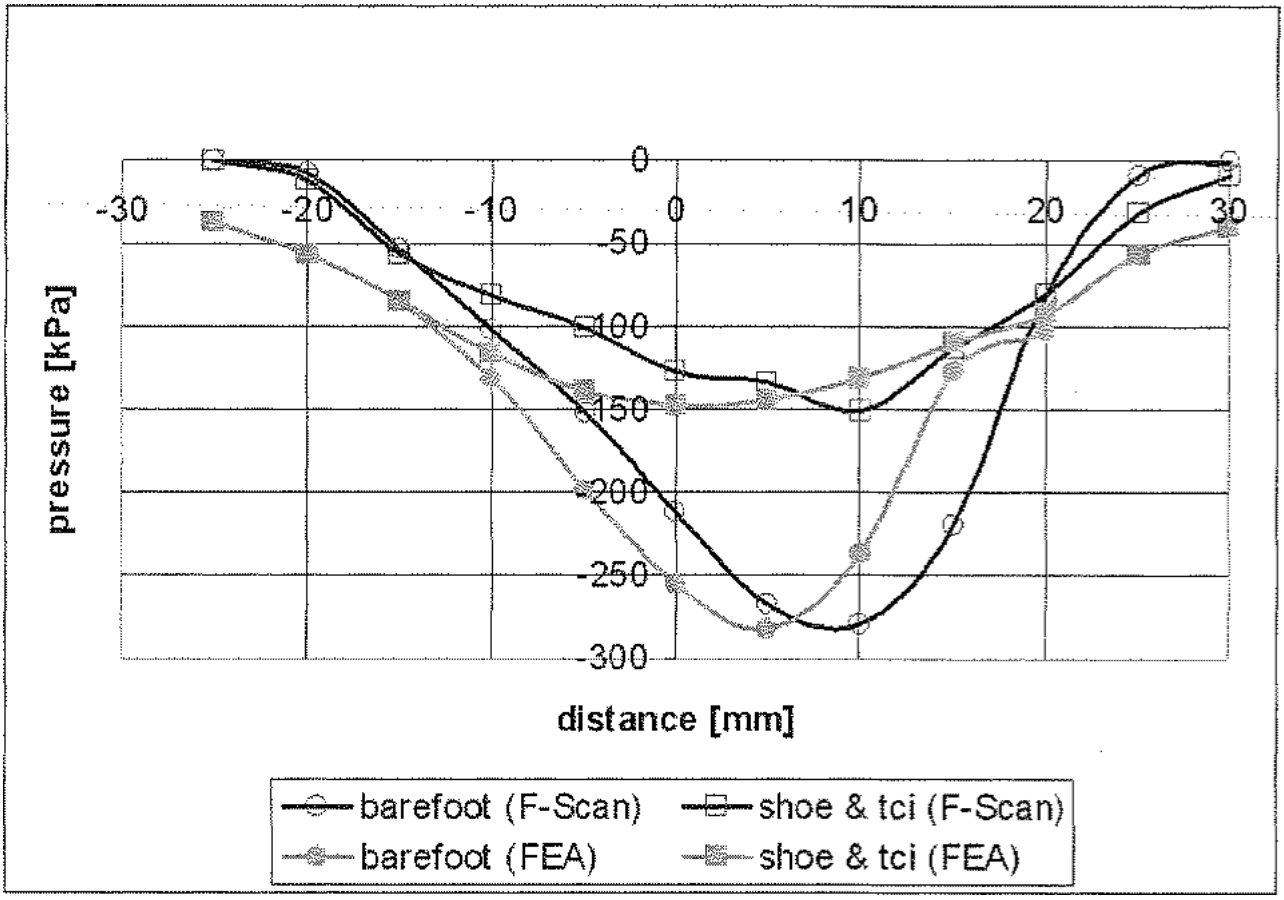

Figure 3.
Pressure distribution for the 2nd ray barefoot and with footwear (therapeutic shoe and standard plastizote #2 TCI) – Fscan vs FEA.

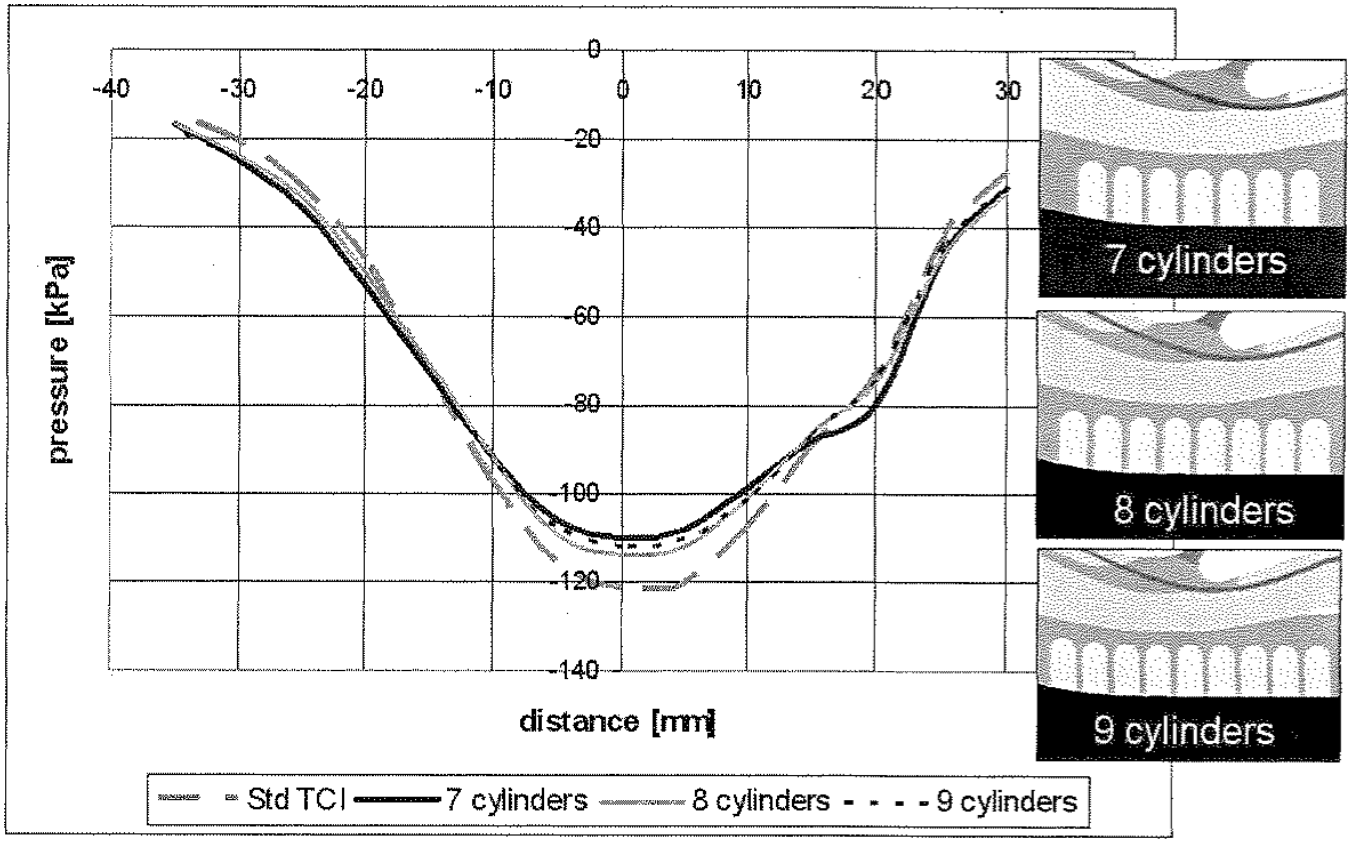

Figure 4.
Pressure distribution from FEA results for different number of cylindrical plugs in the TCI. Sagittal section through the 2nd metatarsal of the diabetic subject.

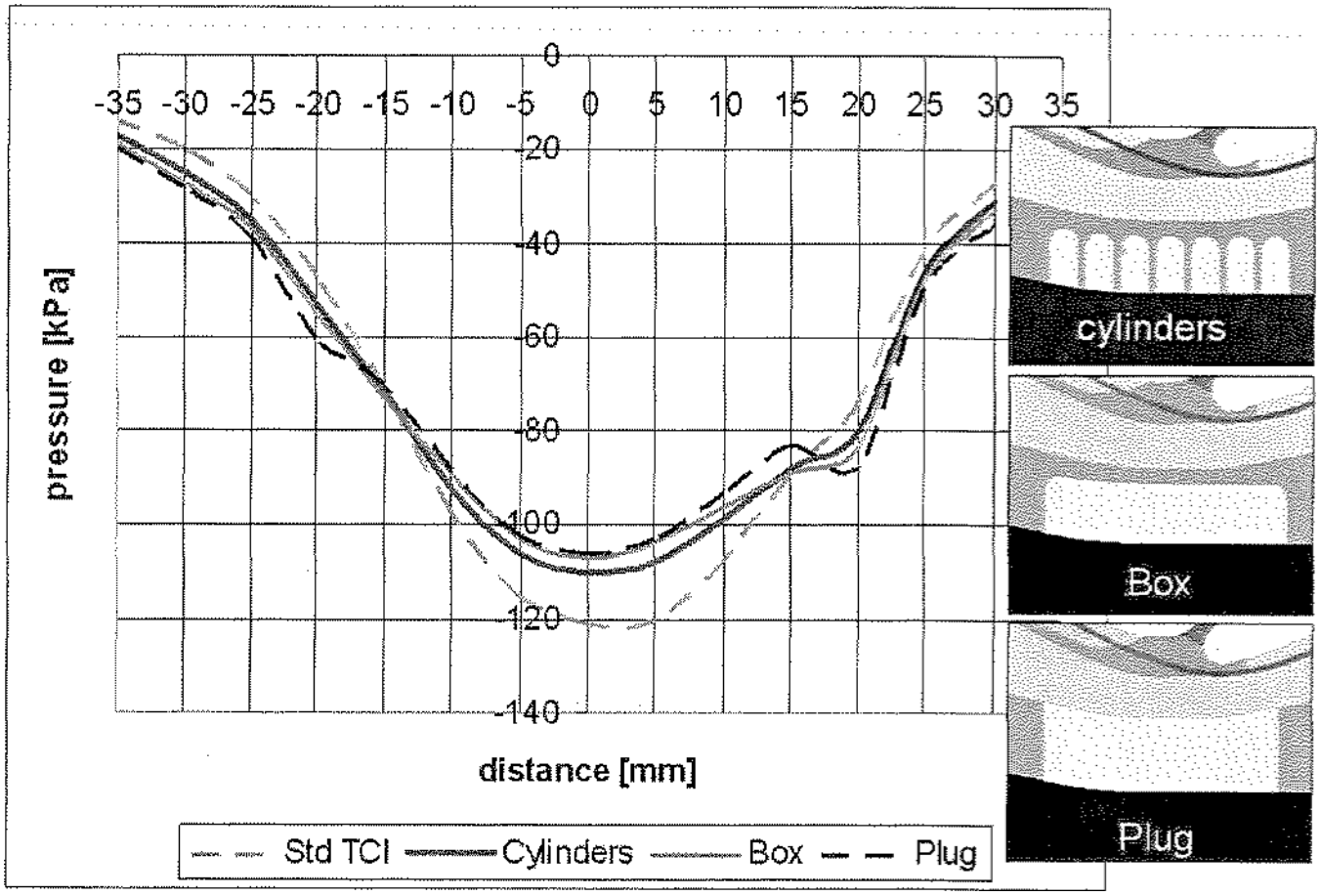

Figure 5.
Pressure distribution from FEA results for different TCI designs. Sagittal section through the 2nd metatarsal of the diabetic subject.

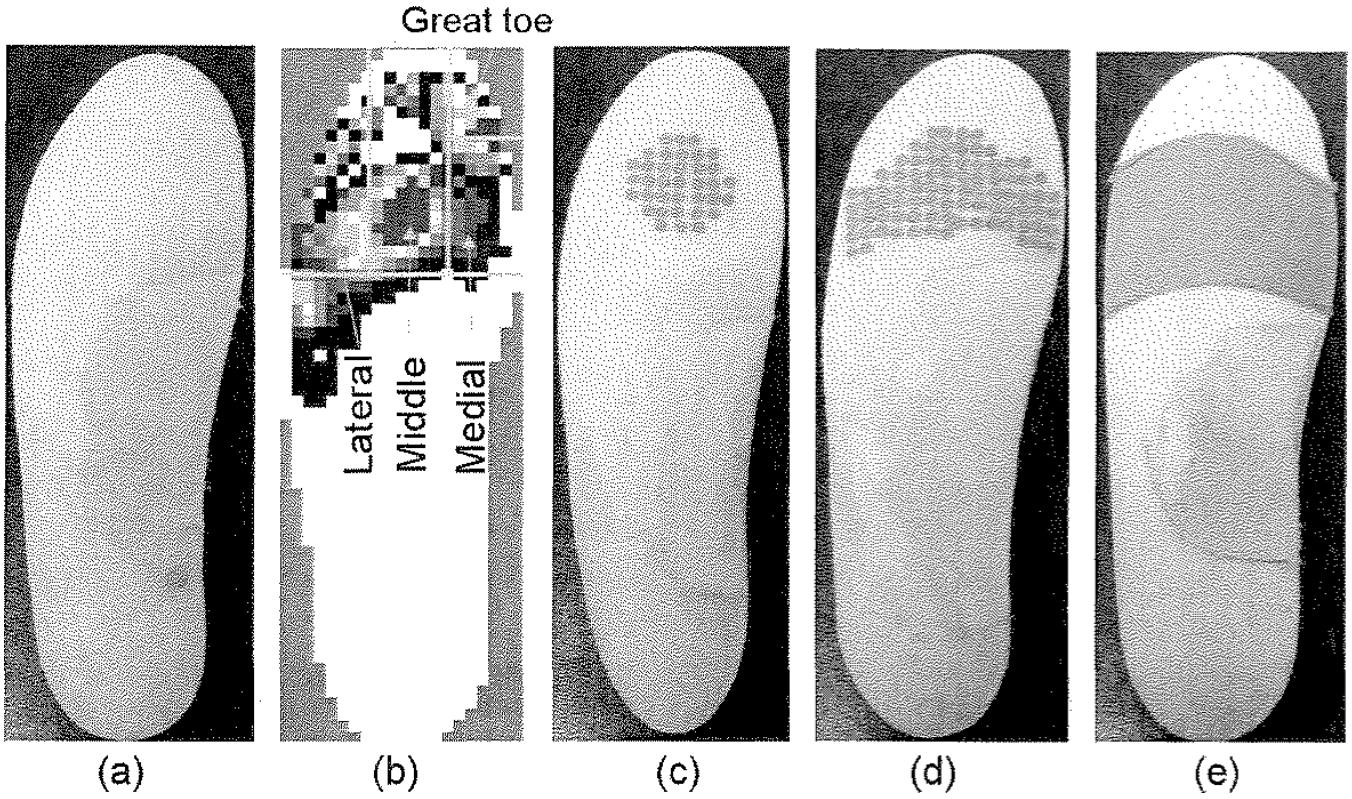

Figure 6.
TCI insoles for the left foot of the subject with forefoot pain. (a) Standard TCI, (b) F-Scan pressure reading during late stance of walking with indication of the four regions of the forefoot where the tabular information was obtained; (c) local plug design; (d) global plug design; (e) inlay design.

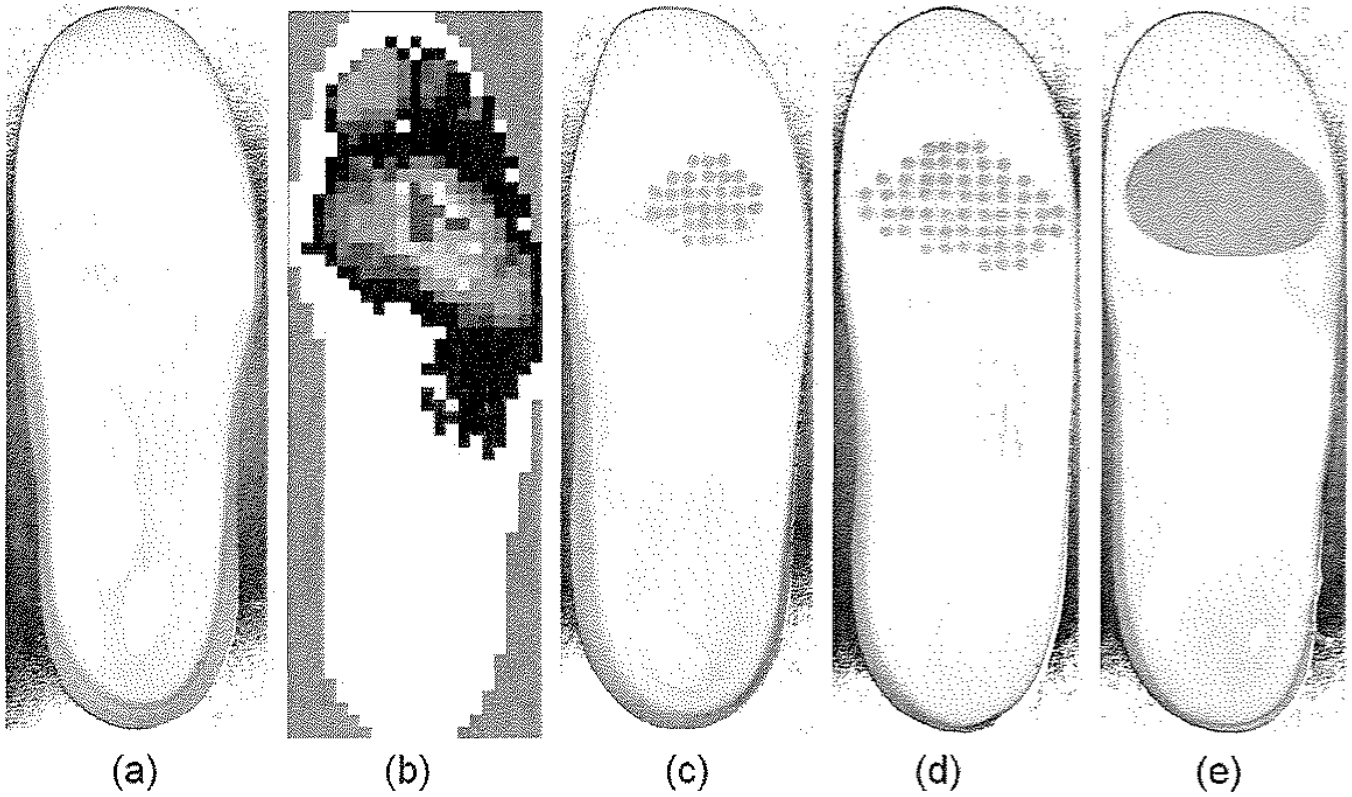

Figure 7.
TCI insoles for the right foot of the diabetic subject. (a) Standard TCI, (b) F-Scan pressure reading during late stance of walking; (c) local plug design; (d) global plug design; (e) inlay design.

Table 1

Peak plantar pressure (PP) for four different regions of the forefoot of the subject without diabetes from the F-Scan measurements. Average PP and standard deviation (STD) values over 18 steps.

Insole	Peak pressure (PP in kPa), standard deviation (STD in kPa) and % change in PP (ΔP) from TCI alone											
	Great toe			Medial			Middle			Lateral		
	PP	STD	ΔP	PP	STD	ΔP	PP	STD	ΔP	PP	STD	ΔP
Standard TCI	337	66	---	176	33	---	427	28	---	174	34	---
Local plug	347	85	3.0	156	38	−11.4	369	38	−13.6	182	43	4.6
Global plug	341	60	1.2	149	33	−15.3	386	36	−9.6	157	25	−9.8
Inlay	391	73	16.0	158	35	−10.2	402	29	−5.9	146	24	−16.1

Table 2

Peak pressure (PP) for four different regions of the forefoot of the diabetic subject from the F-Scan measurements. Average PP and standard deviation (STD) values over 18 steps.

Insole	Peak pressure (PP in kPa), standard deviation (STD in kPa) and % change in PP (ΔP) from TCI alone											
	Great toe			Medial			Middle			Lateral		
	PP	STD	ΔP	PP	STD	ΔP	PP	STD	ΔP	PP	STD	ΔP
Standard TCI	168	57	---	134	54	---	241	35	---	229	58	---
Local plug	198	40	17.8	145	34	8.2	233	22	−3.3	193	34	−15.7
Global plug	224	38	33.3	150	19	11.9	226	31	−6.2	173	36	−24.5
Inlay	202	29	20.2	149	36	11.2	259	14	7.5	220	25	−3.9